
USING SPACE-BASED INFORMATION ABOUT THE EARTH SPACE MONITORING OF NATURAL DISASTERS

Monitoring the State of the Landslide Zone on the Bureya River in 2018–2019 with Radar and Optical Satellite Images

V. G. Bondur^{a,*}, L. N. Zakharova^{a,b,**}, and A. I. Zakharov^{a,b}

^a*AEROCOSMOS Research Institute for Aerospace Monitoring, Moscow, 105064 Russia*

^b*Kotelnikov Institute of Radioengineering and Electronics, Russian Academy of Sciences,
Fryazino Branch, Fryazino, 119991 Russia*

**e-mail: vgbondur@aerocosmos.info*

***e-mail: ludmila@sunclass.ire.rssi.ru*

Received December 9, 2019; revised December 10, 2019; accepted December 11, 2019

Abstract—Results are presented from monitoring the current state of the area of the landslide on the Bureya River in 2018–2019 using images from synthetic aperture radars and optical sensors of the Sentinel multisatellite system. Differential radar interferometry shows the stability of the landslide’s surface in the first four months after the landslide and since the end of July 2019. The small-scale dynamics of the surface are revealed within the landslide circus. It is shown that interferometry cannot be used to observe large modifications of the shoreline, in contrast to optical images, where the effects of the collapse of shoreline fragments and shoreline flooding were clearly observed. Ongoing landslide activity within the landslide circus and area of shoreline collapse is detected using satellite images. Continuous monitoring of this and other dangerous landslide zones on the Bureya River is needed.

Keywords: Bureya River, remote sensing, multisatellite system, optical images, synthetic aperture radar, radar images, radar interferometry, landslide, surface displacements

DOI: 10.1134/S0001433820120361

INTRODUCTION

The growing number of natural disasters and the damage they cause (Bondur et al., 2009; *Prirodnye opasnosti...*, 2000) requires that we develop and use new ways of predicting and monitoring such natural phenomena as earthquakes (Akopyan et al., 2017; Bondur and Zverev, 2005a, 2005b, 2007; Bondur et al., 2007; Bondur and Smirnov, 2005), floods (Bondur et al., 2009; *Prirodnye opasnosti...*, 2000), typhoons (Bondur et al., 2008a, 2008b; 2009), wildfires (Bondur, 2016; Bondur and Ginzburg, 2016; Bondur et al., 2017), and landslides (Bondur et al., 2019a, 2019b, 2019d; Zakharova et al., 2019; Zakharov and Zakharova, 2019; Zakharova and Zakharov, 2019; Kramareva et al., 2018, 2019).

These problems can be solved using satellite remote sensing, particularly all-weather radar in combination with optical means (Bondur, 2011; Bondur et al., 2009; 2019a, 2019b, 2019c, 2019d; Zakharov and Zakharova, 2019; Zakharova and Zakharov, 2019; Zakharova et al., 2019; Bondur and Chimitdorzhiev, 2008a, 2008b; Bondur et al., 2019c; Bondur and Starchenkov, 2001; Bamler and Hartl, 1998; Colesanti and Wasowski, 2006).

In this work, we consider the use of remote sensing to monitor landslide processes on the Bureya River in 2019 after a landslide in December 2018.

The catastrophic landslide on the bank of the Bureya River on December 11, 2018, blocked the channel of the Bureya River and required not only immediate measures to remove the blockage, which threatened the flooding and destruction of human settlements and economic infrastructure, but the organization of landslide zone monitoring to determine the history and current dynamics of this dangerous natural phenomenon as well.

Ground-based field studies since the beginning of 2019 have provided insight into the extent of the landslide (Pererva et al., 2019). They were invaluable in organizing and implementing efforts to scour a hole in the river channel in late January–early February 2019. However, qualitatively new and detailed data on the state of the landslide zone, and on the history of the landslide’s development and current dynamics, can be obtained only through satellite optical and radar observations.

The first data on the extent of the landslide event on the Bureya River were obtained from an optical image produced by the Sentinel-2B satellite on December 12, 2018 at 02:22 UT (Kramareva et al., 2018). This satellite image showed the zone of collapse and the resulting embankment, which blocked the river channel. Zones of the damage of the shoreline

forest cover by a wave resulting from the soil collapsing into the water were also identified. The dynamics of creating the hole in the blockage by blasting in late January–early February 2019 and its erosion by high water until the end of April 2019 was observed using optical survey data from the Sentinel-2 satellites and the International Space Station (Kramareva et al., 2019, Ostroukhov et al., 2019).

Radar images from Sentinel-1 satellites were first used to monitor the winter landslide activity from 2017 to 2018 in (Zakharova and Zakharov, 2019). Zakharova et al. (2019) analyzed the consequences of the landslide, giving an estimate of its size and the volume of removed soil, along with the stability of the landslide zone in winter 2019. Radar images obtained from the ALOS-1 and ALOS-2 satellites allowed us to observe the development of the landslide from 2006 to 2017 via radar interferometry (Bondur et al., 2019a, 2019b).

In this work, we present results from monitoring the state of the landslide area on the Bureya River using optical and radar survey data from the Sentinel-1A/B and Sentinel-2A/B satellites.

USING SATELLITE IMAGES

The satellite images we used in this work were obtained from the Sentinel-2A/B satellites, which share the same sun-synchronous orbit with a 180° orbital phasing difference at the altitude of 798 km.

The Sentinel multisatellite system was created by the European Space Agency as part of the Copernicus Global Space Monitoring Project. Optical surveys are performed in 13 spectral bands within the 443–2190 nm band at a resolution of 10/20/60 m with coverage of 290 km (http://esamultimedia.esa.int/docs/S2-Data_Sheet.pdf). The interval between repeated surveys is 2–3 days at the latitude of the landslide area.

The Sentinel-1A/B satellites provide radar images of the Earth's surface using synthetic aperture radars (SARs) in the C-band (wavelength, 5.6 cm) from a sun-synchronous orbit with an altitude of 693 km. The southern part of Russia's Far Eastern Federal District with the Bureya River is surveyed on the descending part of the orbit with repeat cycle of 12 days in the IW (interferometric wide) mode, which can be used for interferometric topographic measurements or analyzing the dynamics of the underlying surface. The survey is conducted at right looking flight attitude in wide-swath mode with 240 km swath width. The pixel spacing of SLC SAR image is 2.3 m in slant range and 14.1 m in azimuth (<https://sentinel.esa.int/web/sentinel/missions/sentinel-1/overview>).

In this work, we used a series of satellite radar images obtained from relative orbits 61 and 134.

Optical images from the Sentinel-2A/B satellites are preferred for observing large-scale changes in relief, since they have a better spatial resolution, no

speckle noise (which is characteristic of SARs), and allow good visual perception.

RESULTS AND DISCUSSION

Figure 1 shows fragments of optical images obtained from the Sentinel 2A/B satellites from December 12, 2018 to July 26, 2019.

Figure 1a shows a fragment of an optical satellite image of the landslide area, obtained on December 12, 2018, by the Sentinel-2 satellite shortly after the collapse. It is difficult to differentiate the river channel and collapse zone in the shadow of the high southern bank, due to the low winter sun. The main changes on the Earth's surface that were observed in satellite optical images after the landslide were

(1) the formation of a hole from blasting in late January–early February 2019 (indicated by the arrow in Fig. 1b);

(2) the collapse/flooding of the walls of the hole in April 2019 during the flood;

(3) the large-scale collapse of the shoreline from May 3 to May 11, 2019 (the arrow in Fig. 1c); and

(4) the flooding of part of the shoreline area of the landslide zone, due to a rise in the level of the river's water from 21 to 26 July 2019 (the arrow in Fig. 1d).

Radio interferometric monitoring from repeated orbits of the Sentinel-1 satellites allowed us to detect small-scale (radar wavelength) deformations of the underlying surface that appeared during the period between the surveys. The coherence of the backscattered signals of radar survey sessions that form an interferometric pair is a key condition for detecting and measuring displacements of the Earth's surface from the phase difference in the interferogram (Zakharov and Zakharova, 2019).

A disadvantage of using Sentinel-1 SAR (C-band) radio interferometric observations of the Earth's surface covered with dense forest vegetation is a high temporal decorrelation between signals obtained in neighboring surveys during the warm season (Bondur et al., 2019c; Bondur and Chimitdorzhiev, 2008a, 2008b). We can measure the elevation and observe displacements of the forest cover in this frequency band only under conditions of negative air temperature (i.e., under conditions of greater temporal stability of the dielectric properties of frozen tree crowns) (Zakharova and Zakharov, 2019).

A specialty of the observations of the landslide area in 2019 is that the scattering surface was free of vegetation, as was shown in (Bondur et al., 2019a). This results in higher coherence in the area as compared with the surrounding forested surface.

Figure 2 shows the coherence plots of the landslide area and adjacent forest for the period from November 16, 2018 to October 5, 2019. The interval

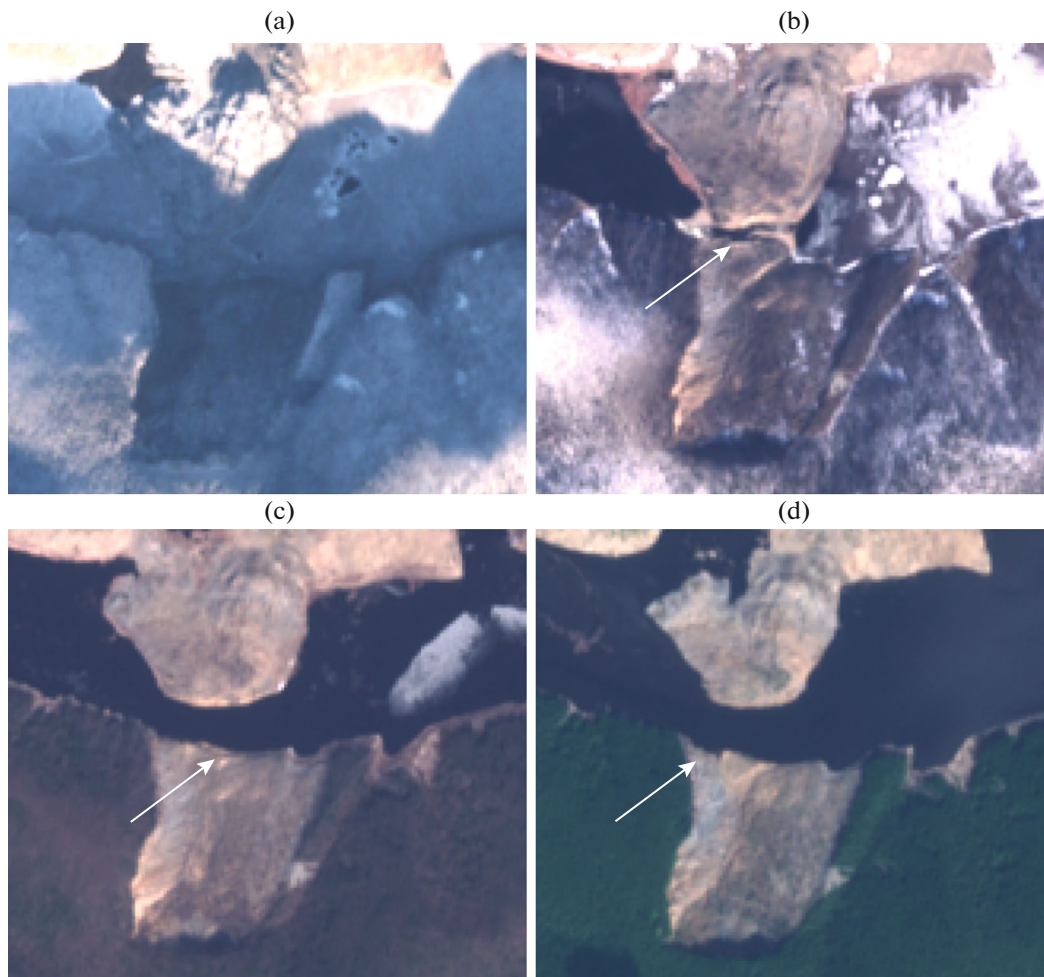


Fig. 1. Optical images from the Sentinel-2 satellite in the Bureya landslide zone.

between the surveys of radar image pairs was determined by the 12-day orbit repeat cycle.

The high coherence of backscattered signals from the forest area until the end of March 2019 is explained by a high stability of its dielectric properties at negative air temperatures (Bondur et al., 2019c; Bondur and Chimitdorzhiev, 2008a, 2008b). It should be noted that the large-scale displacements of surface fragments with amplitudes of more than half the wavelength in an image pixel leads to the decorrelation of the signals from these image pixels of the interferometric pair (Bondur et al., 2019c).

The poor coherence of the backscattered signals for the landslide area until December 12, 2018 can therefore be explained by the sudden activation of relatively large-scale displacements of the landslide surface prior to the collapse. The coherence of the backscattered signals from of the landslide surface was low in April–early May 2019 due to snow melting and changes in soil moisture on the southern shoreline slope during this period. Unusually frequent and heavy rains in May–June, the intensity of which fell

only at the beginning of July 2019 (Pererva et al., 2019), could also have been responsible for the low coherence and poor quality of interferometric observations in these months. The low coherence of the interferometric pair from August 7, 2019 to August 19, 2019 (see Fig. 2) is also explained by intense precipitation (immediately prior to the first survey during this period) (www.rp5.ru).

Figure 3 presents a set of some coherence maps of radar signals within the landslide zone in the spring–summer period of 2019. The light tones correspond to better coherence. The high coherence of radar signals characteristic of the northern bank of the Bureya River, including areas along the banks of the Middle Sandar River, is explained by higher stability of the open surface of the shoreline zone, where vegetation was swept away by a tsunami-like wave in December 2018. The gradual drying of the soil of the landslide circus resulted in a rise in the coherence of radar signals, allowing us to search for signs of small surface displacements since July 2019 using radar interferometry.

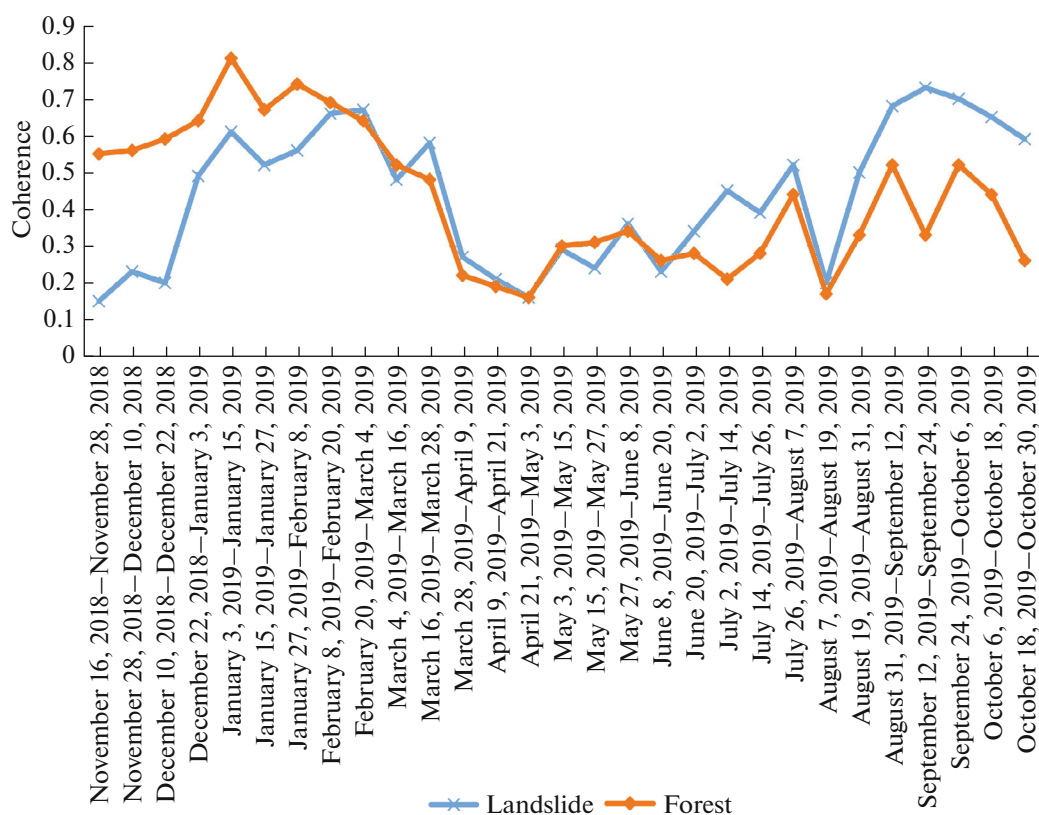


Fig. 2. Coherence of reflected signals from the landslide zone and adjacent forest area for the period from November 16, 2018 to October 5, 2019.

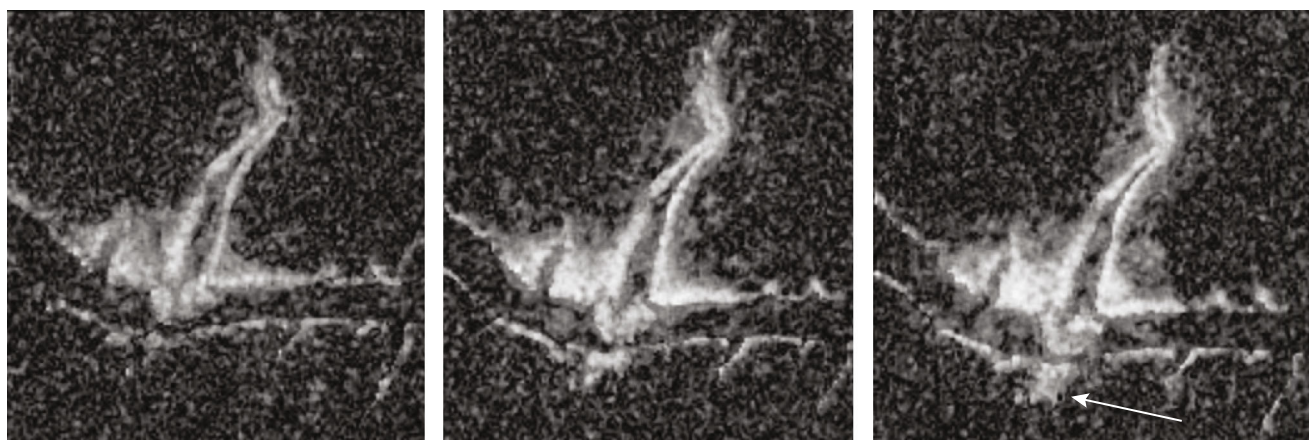


Fig. 3. Coherence of radar signals for a part of the Earth's surface in May, June, and July 2019. The arrow indicates the landslide zone.

The search for small-scale dynamics on the surface of the Bureya landslide circus since the end of 2018 (immediately after the collapse) by means of differential radar interferometry has been a subject of study (Zakharova et al., 2019). As is known, the interferometric phase on a radar interferogram depends mainly on variations in relief heights (the so-called topographic phase), and on local displacements of the scattering sur-

face during the period between surveys of the interferometric pair (Bamler and Hartl, 1998). When there is a digital elevation model (DEM), the influence of the topographic phase can be compensated for with subsequent determining phase displacements on the interferograms caused by the dynamics of the scattering surface.

Our differential interferograms according to Sentinel-1 satellite data were based on an SRTM DEM that

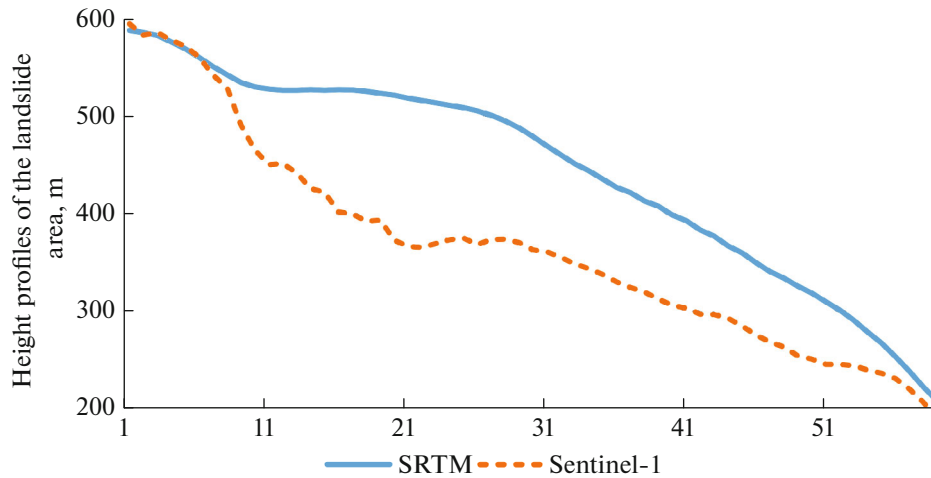


Fig. 4. Height profile according to SRTM data (solid line) and Sentinel-1 interferometric survey data (dashed line).

represented the elevations of the entire scene of the radar image fairly well, except for the landslide zone, where the landscape changed.

Figure 4 shows the profile of the surface heights of the landslide area along the slope, computed according to the Sentinel-1 interferometric survey in January 2019 (dashed line), and one derived from the SRTM DEM (solid line). The vertical axis is the height above the sea level in meters, and the horizontal axis shows the profile samples (pixels). The pixel spacing on the surface is around 14 m.

The maximum difference between the true surface height and the height according to the SRTM DEM is as great as 150 m. Such errors in the relief heights can be falsely interpreted as surface displacements with fairly large amplitudes. This topographic phase, generated by the difference between the SRTM DEM and true surface topography, was compensated for in a phase measured by several means (Zakharov and Zakharova, 2019).

Analysis of a series of eight 12-day differential interferograms from the end of December 2018 to the beginning of April 2019 revealed no dynamics of the landslide area surface either within the circus or on the adjacent slopes. Blasting operations from the third decade of January to the first decade of February in 2019 produced no noticeable (more than 1–2 mm) soil displacements on the landslide slope either.

Examples of interferograms with surface subsidence are shown in Fig. 5, along with the respective fragments of the radar and optical images. According to the interferometric processing chain used in this work, the lighter tones within the landslide correspond to the sliding of the reflecting surface from the satellite down the landslide slope.

The first interferograms after the three-month period of low coherence, formed from the data acquired in July (Fig. 5a), did not allow us to assess the pattern

of displacements caused by the noisy phase image clearly, especially in the upper part of the landslide circus (its southern edge).

Reliably measured signs of rockslide displacements on the circus surface with the maximum line-of-sight displacement of 0.7 cm were revealed in the middle eastern part of the landslide in late August 2019 (Fig. 5b). Figure 5c shows the soil displacement throughout the eastern edge of the landslide and near the main scarp. Figure 5d shows a wide light band that marks a displacement in the middle part of the landslide (corresponded to pixels 26–31 of the profile given in Fig. 4). This band crosses the zone of the landslide circus from its western to its eastern edge.

Table 1 provides a detailed description of the results of observations of the small-scale dynamics of the surface within the landslide circus on the Bureya River from July to mid-October 2019.

Analysis of Table 1 indicates both the temporal and spatial irregularity of circus surface displacement. In July–August 2019, displacements were most often recorded at the eastern edge of the landslide circus at an amplitude of up to 1.5 cm along the line of sight. The dynamics grew in the upper part of the circus after mid-September 2019 (pixels 6–16 of the height profile in Fig. 4).

CONCLUSIONS

The results of monitoring the landslide area on the Bureya River bank in 2018–2019 by means of spaceborne radar and optical observations demonstrated the high information content of satellite remote sensing, which allowed us to reveal small-scale dynamics of the Earth's surface in the landslide area. SAR interferometry was used to study the stability of the landslide circus's surface and adjacent shoreline slopes at the

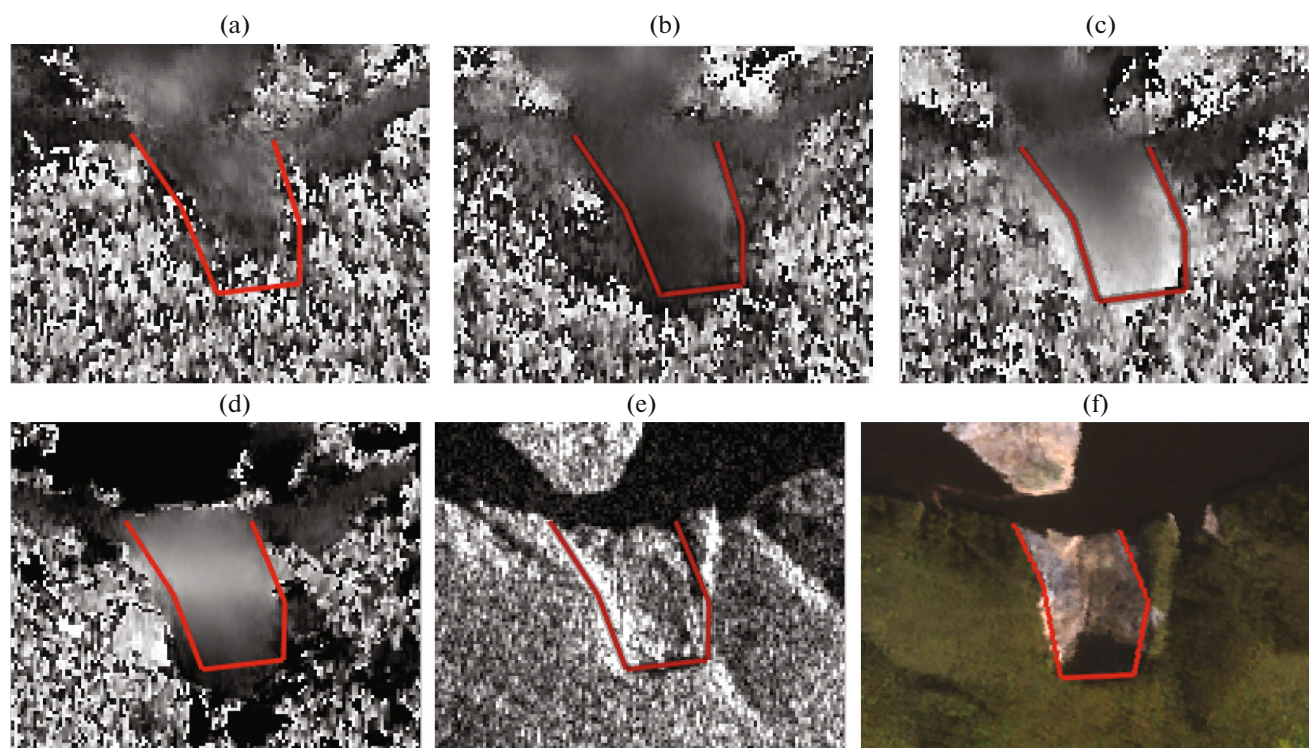


Fig. 5. Examples of (a–d) interferograms and (e–f) satellite images for the landslide zone, according to the Sentinel-1 SAR survey data in the third quarter of 2019 with the contour of the landslide zone: (a) July 9, 2019–July 21, 2019; (b) August 26, 2019–September 7, 2019; (c) September 7, 2019–September 19, 2019; (d) September 19, 2019–October 1, 2019; (e) radar image obtained on September 19, 2019; and (f) optical image obtained on September 25, 2019.

beginning of 2019, including the period of blasting to scour the hole.

The radar interferometric data from the Sentinel-1 satellites proved to be of no use for observing local shoreline collapses, unlike the optical images from Sentinel-2 satellites with clearly visible effects of the collapse of shoreline fragments and shoreline flooding.

The first signs of the displacements of rock debris fragments on the sliding surface in different parts of the landslide circus were detected in late July 2019. The displacements continued to be detected until the end of the observation period (mid-October 2019). Large-scale displacements/collapses that would result in loss of the interferometric coherence and be

Table 1. Surface displacements observed within the landslide circus on the Bureya River in July–October 2019

Dates	Maximum line-of-sight displacement over 12 days	Position of maximum displacement
July 9, 2019–July 21, 2019	0.5 cm	Eastern edge, middle–bottom
July 21, 2019–August 2, 2019	1.4 cm	Eastern edge, middle–bottom
August 2, 2019–August 14, 2019	0.7 cm	Eastern edge, middle–bottom
August 14, 2019–August 26, 2019	0.4 cm	Eastern edge
August 26, 2019–September 7, 2019	0.5 cm	Eastern edge, middle
September 7, 2019–September 19, 2019	1.9 cm	Eastern edge and main scarp
September 19, 2019–October 1, 2019	1.4 cm	Band in middle part
October 1, 2019–October 13, 2019	1.5 cm	Upper part of the landslide

visible on optical images were not detected within the circus.

The identified zone of the ongoing landslide activity within the landslide circus and shoreline collapse requires continuous monitoring of this and other dangerous landslide zones on the Bureya River.

ACKNOWLEDGMENTS

The authors are grateful to the European Space Agency for providing Sentinel-1 and Sentinel-2 data.

FUNDING

This work was performed as part of a State Assignment for the organizations participating in it. It was supported by the Russian Foundation for Basic Research, project no. 18-07-00816; and by the RF Ministry of Education and Science, project no. RFMEFI60719X0306.

REFERENCES

- Akopyan, S.Ts., Bondur, V.G., and Rogozhin, E.A., Technology for monitoring and forecasting strong earthquakes in Russia with the use of the seismic entropy method, *Izv., Phys. Solid Earth*, 2017, vol. 53, no. 1, pp. 32–51.
<https://doi.org/10.1134/S1069351317010025>
- Bamler, R. and Hartl, P., Synthetic aperture radar interferometry, *Inverse Probl.*, 1998, vol. 14, pp. R1–R54.
- Bondur, V.G., Aerospace methods and technologies for monitoring oil and gas areas and facilities, *Izv., Atmos. Ocean. Phys.*, 2011, vol. 47, no. 9, pp. 1007–1018.
- Bondur, V.G., Satellite monitoring of trace gas and aerosol emissions during wildfires in Russia, *Izv., Atmos. Ocean. Phys.*, 2016, vol. 52, no. 9, pp. 1078–1091.
<https://doi.org/10.1134/S0001433816090103>
- Bondur, V.G. and Chimitdorzhiev, T.N., Texture analysis of radar images of vegetation, *Izv. Vyssh. Uchebn. Zaved., Geod. Aerofotos'emka*, 2008a, no. 5, pp. 9–14.
- Bondur, V.G. and Chimitdorzhiev, T.N., Remote sensing of vegetation by optical microwave methods, *Izv. Vyssh. Uchebn. Zaved., Geod. Aerofotos'emka*, 2008b, no. 6, pp. 64–73.
- Bondur, V.G. and Ginzburg, A.S., Emission of carbon-bearing gases and aerosols from natural fires on the territory of Russia based on space monitoring, *Dokl. Earth Sci.*, 2016, vol. 466, no. 2, pp. 148–152.
<https://doi.org/10.1134/S1028334X16020045>
- Bondur, V.G. and Smirnov, V.M., Method for monitoring seismically hazardous territories by ionospheric variations recorded by satellite navigation systems, *Dokl. Earth Sci.*, 2005, vol. 403, no. 5, pp. 736–740.
- Bondur, V.G. and Starchenkov, S.A., Methods and programs for processing and classification of aerospace images, *Izv. Vyssh. Uchebn. Zaved., Geod. Aerofotos'emka*, 2001, no. 3, pp. 118–143.
- Bondur, V.G. and Zverev, A.T., Satellite method of earthquake forecast based on the analysis of lineament system dynamics, *Issled. Zemli Kosmosa*, 2005a, no. 3, pp. 37–52.
- Bondur, V.G. and Zverev, A.T., A method of earthquake forecast based on the lineament analysis of satellite images, *Dokl. Earth Sci.*, 2005b, vol. 402, no. 4, pp. 561–567.
- Bondur, V.G. and Zverev, A.T., Lineament system formation mechanisms recorded in space images during the monitoring of seismic hazard areas, *Issled. Zemli Kosmosa*, 2007, no. 1, pp. 47–56.
- Bondur, V.G., Garagash, I.A., Gokhberg, M.B., Lapshin, V.M., Nechaev, Yu.V., Steblov, G.M., and Shalimov, S.L., Geomechanical models and ionospheric variations related to strongest earthquakes and weak influence of atmospheric pressure gradients, *Dokl. Earth Sci.*, 2007, vol. 414, no. 1, pp. 666–669.
- Bondur, V.G., Pulinets, S.A., and Kim, G.A., Role of variations in galactic cosmic rays in tropical cyclogenesis: Evidence of hurricane Katrina, *Dokl. Earth Sci.*, 2008a, vol. 422, pp. 1124–1128.
- Bondur, V.G., Pulinets, S.A., and Uzunov, D., The effect of large-scale atmospheric vortex processes on the ionosphere using hurricane Katrina as an example, *Issled. Zemli Kosmosa*, 2008b, no. 6, pp. 3–11.
- Bondur, V.G., Krapivin, V.F., and Savinykh, V.P., *Monitoring i prognozirovanie prirodnykh katastrof* (Monitoring and Forecast of Natural Catastrophes), Moscow: Nauchnyi mir, 2009.
- Bondur, V.G., Gordo, K.A., and Kladov, V.L., Spacetime distributions of wildfire areas and emissions of carbon-containing gases and aerosols in northern Eurasia according to satellite-monitoring data, *Izv., Atmos. Ocean. Phys.*, 2017, vol. 53, no. 9, pp. 859–874.
<https://doi.org/10.1134/S0001433817090055>
- Bondur, V.G., Zakharova, L.N., Zakharov, A.I., et al., Long-term monitoring of landslide on the Bureya River bank according to interferometric L-band radar data, *Sovrem. Probl. Distantionnogo Zondirovaniya Zemli Kosmosa*, 2019a, vol. 16, no. 5, pp. 113–119.
- Bondur, V.G., Zakharova, L.N., Zakharov, A.I., Chimitdorzhiev, T.N., Dmitriev, A.V., and Dagurov, P.N., Monitoring of landslide processes by means of L-band radar interferometric observations: the case of Bureya River, *Issled. Zemli Kosmosa*, 2019b, no. 5, pp. 3–14.
- Bondur, V.G., Chimitdorzhiev, T.N., Dmitriev, A.V., and Dagurov, P.N., Assessment of spatial anisotropy of forest vegetation heterogeneity at various azimuth angles of radar polarimetric sensing, *Issled. Zemli Kosmosa*, 2019c, no. 3, pp. 92–103.
<https://doi.org/10.31857/S0205-96142019392-103>
- Bondur, V.G., Chimitdorzhiev, T.N., Dmitriev, A.V., Dagurov, P.N., Zakharov, A.I., and Zakharova, L.N., Radar polarimetry methods for monitoring the changes in backscattering mechanisms in landslide zones for the case study of the bureya river bank collapse, *Issled. Zemli Kosmosa*, 2019d, no. 4, pp. 3–17.
<https://doi.org/10.31857/S0205-9614201943-17>
- Colesanti, C. and Wasowski, J., Investigating landslides with spaceborne synthetic aperture radar (SAR) interferometry, *Eng. Geol.*, 2006, vol. 88, pp. 173–199.
http://esamultimedia.esa.int/docs/S2-Data_Sheet.pdf
<https://sentinel.esa.int/web/sentinel/missions/sentinel-1/overview>
<http://www.rp5.ru>

- Kramareva, L.S., Lupyan, E.A., Amel'chenko, Yu.A., Burtsev, M.A., Krashennnikova, Yu.S., Sukhanova, V.V., and Shamilova, Yu.A., Observation of the hill collapse zone near the Bureya River on December 11, 2018, *Sovrem. Probl. Distantionnogo Zondirovaniya Zemli Kosmosa*, 2018, pp. 266–271.
- Kramareva, L.S., Lupyan, E.A., Amel'chenko, Yu.A., Burtsev, M.A., Krashennnikova, Yu.S., Sukhanova, V.V., Shamilova, Yu.A., and Boroditskaya, A.V., Observing the progress of blasting operations and channeling in the area of the rock slide on the Bureya River, *Sovrem. Probl. Distantionnogo Zondirovaniya Zemli Kosmosa*, 2019, vol. 16, no. 1, pp. 259–265.
- Ostroukhov, A.V., Kim, V.I., and Makhinov, A.N., Estimation of the morphometric parameters of the landslide on the Bureya Reservoir and its consequences on the basis of remote sensing data and field measurements, *Sovrem. Probl. Distantionnogo Zondirovaniya Zemli Kosmosa*, 2019, vol. 16, no. 1, pp. 254–258.
- Pererva, N.I., Davidenko, A.N., and Amel'chenko, Yu.A., Analysis of the causes of the rain floods formation in the Bureya River basin in May–June 2019, *Sovrem. Probl. Distantionnogo Zondirovaniya Zemli Kosmosa*, 2019, vol. 16, no. 4, pp. 303–306.
- Prirodnye opasnosti Rossii* (Natural Hazards in Russia), Moscow: KRUK, 2000.
- Zakharov, A.I. and Zakharova, L.N., The potential of phase measurements in radar interferometry for the observation of emergency situations: the case of the Bureya landslide, *Radioelectron. Nanosyst. Inf. Tekhnol.*, 2019a, vol. 11, no. 1, pp. 31–38.
<https://doi.org/10.17725/rensit.2019.11.031>
- Zakharova, L.N. and Zakharov, A.I., Interferometric observation of landslide area dynamics on the Bureya River by means of Sentinel-1 radar data in 2017–2018, *Sovrem. Probl. Distantionnogo Zondirovaniya Zemli Kosmosa*, 2019b, vol. 16, no. 2, pp. 273–277.
- Zakharova, L.N., Zakharov, A.I., and Mitnik, L.M., First results of radar monitoring of the landslide consequences on the Bureya riverbank using Sentinel-1 data, *Sovrem. Probl. Distantionnogo Zondirovaniya Zemli Kosmosa*, 2019, vol. 16, no. 2, pp. 69–74.

Translated by D. Zabolotny